Quest Journals
Journal of Research in Environmental and Earth Sciences
Volume 7 ~ Issue 6 (2021) pp: 16-23
ISSN(Online) :2348-2532
www.questjournals.org

Research Paper

Assessment of Water Stress in Plants Using Image Processing For Tiruvallur Taluk of Tamil Nadu

Anitha K
Department of Electronics and Communication Engineering, Sri Chandrasekharendra Saraswathi Viswa Mahavidyalaya, Kanchipuram – 631561.
Corresponding Author: K.Anitha

ABSTRACT: *Assessment of plant water stress is required for the management of large areas like agriculture fields and forest. The photosynthetic potential of a plant is an essential parameter of waters stress. The growth, productivity and conditions of plant health depend purely on the water stress or moisture index. Manual moisture measurement is a cumbersome method for a wide region. The latest remote sensing technology has been sufficiently useful to estimate the plants' moisture index. Recent Sentinel -2 satellite imaging has been obtained from NASA for the Thiruvallur Taluk research area of Tamil Nadu, India. The total area covered by the report is 663 km2. This analysis evaluated the four classes of the humidity index area, i.e. extremely high, very high, mild, least, using the Open Source software image processing tool. The ranges are 0,2-0,3%, 0,3-0,4%, 0,4-0,5%. The same is said for the description that the region covering the vegetation index spectrum of 0.5-0.6, 0.6-0.7, 0,7-0.8 and 8505 ha (12.77 percent), 3,212 ha (4.82 percent), 29 ha (0,04 percent). The land area 34602 ha (51.94%), 19158 ha (28.76%) and 11934 ha (17.91%) cover the moisture content of 0.0-0.1, 0.1-0.2, and 0.2-0.3, respectively. The maximum of 917 ha (1.377%) has high amount of moisture content.*

KEYWORDS: *Image processing, Moisture content, Satellite Imagery, Tiruvallur Taluk*

Received 25 May, 2021; Revised: 06 June, 2021; Accepted 08 June, 2021 © The author(s) 2021. Published with open access at www.questjournals.org

I. INTRODUCTION

The scientific literature extensively describes the use of remote sensing technology and spectral reflection data to measure spatial patterns of plant water tension. The spectral responses of vegetation to plant stress are usually studied using airborne, space and handheld Remote Sensing technologies [1].

Remote sensing technology offers an objective and consistent way of measuring plant stress and is able to record important spectral data over a visible spectrum (400-700 nm) in longer wavelengths. Different methods were studied for detecting plant water tension, such as plant activity, movement of leaf tips to detect the emergence of wilt, canopy temperature and plant w. plant The impacts on the geometrical feature of the leaf and weather such as leaf angle, air temperature and moisture as well as wind remain challenges [2].

Plant pigments such as chlorophyll and xanthophyll absorb the most radiant radiant in the visible band yet display the greater radiance in the NIR. The reflective pattern changes due to a reduction in the efficacy of photosynthetic absorption and leads to increased reflections in the visible band and a decline in the NIR band[1] . The combination of data from spectral bands to NIR/Red or(NIR – Red)/(NIR + Red) indices thus amplifies spectrum disparities and offers supplementary information for stress detection .[3]

The repeated occurrence in various parts of the globe of intense fires over the past two decades has shown that realistic methods to monitor these occurrences need to be established and eventually alleviated [1]. Study on biomass burning has progressed from satellite data recording on active fires . The NDMI is the remote sensor index for the estimation of the canopy level of leaf water[2]. The NDMI is a regular index of sensors.

II. STUDY AREA

The field under analysis occupies the longitude from 79.75 E to 80.10E and latitude fr[4]om 12.945N to 13.32N. In the southern Tamil of Nadu, Tiruvallur is a fast-developing district. The total study area covers 666.5 $km^{2,}$ and It has a great industrial and commercial significance, as Tiruvallur Taluka near the town of Chennai. The topographic sheet of the study area is shown in Figure 1. The presence of Tamil Nadu's state further emphasises the strategic importance of the Tiruvallur district through the existence of many academic institutions and development units, commercial institutions, religious monuments, and temples. The tropical

climate is the Min 13.9 °C and Max 45°C temperate climate [3]. The region has three sections: (1) Pulicat Lak is on the north shore of Tiruvallur and is India's second-largest brackish lake, and the Ennore port and North thermal power plants are two major industries. Fishing, croplands and salt production rely on the north Tiruvallur coast. 2) Industrial waste disposal from the EID Parry, MRF piping factory, Ennore thermal power plant, Manali petroleum company Tiruvallur, Tamil Nadu petro goods and SPIC petrol producing plants shall take place along the Central Coast of Tiruvallur. 2) A large number of animals and thus visitors attract this mangrove area.

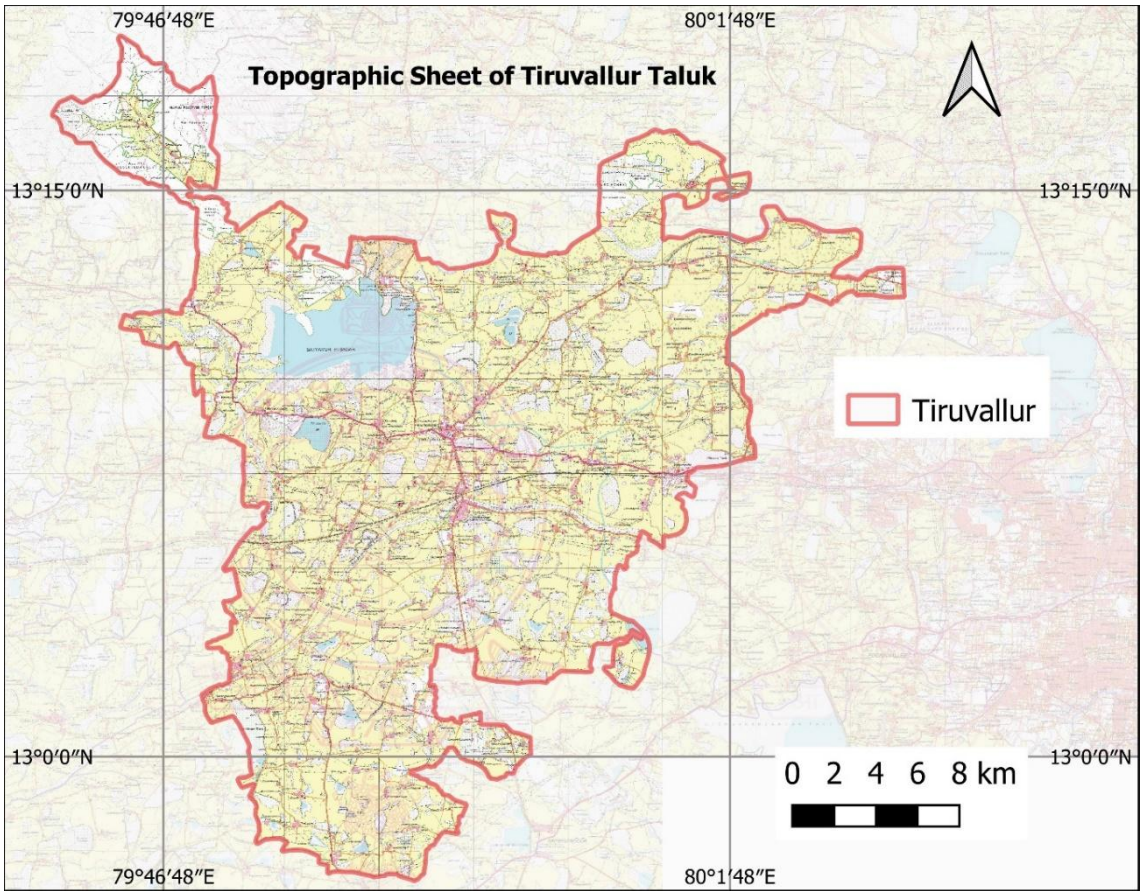

Figure 1: Topographic map of Tiruvallur Taluk, Tamil Nadu, India

III. METHODOLOGY

The Near-Infrared (NIR) and Short-Wave Infrared (SWIR) channels are a satellite index of the Standardised Difference Water Index (NDMI).

A. Data Collection

Sentinel-2 satellite aims to observe the land and the mission consists of two satellites that provide high-resolution optical images. The surveillance targets include vegetation, soil and coastal areas. In June 2015, the first satellite, Sentinel 2 was launched [5]–[7]. Sentinel-2 is a Copernicus Program Earth Observation Project that systemically obtains high-spatial (10 m to 60 m) optical imagery across land and coastal waters. The constellation consists of two double satellites, Sentinel-2A and Sentinel-2B. The mission promotes various activities, including farm inspection, emergency response, land cover classification, and water quality. The mission supports Sentinel-2 is intended for a wide variety of terrestrial and marine water uses. The mission will provide information on farming and forestry activities and food security management. Satellite images are used to assess different plant indicators, including chlorophyll leaf area and water content indexes [8]–[10]. For successful prediction of yield and applications related to the world's vegetation, this is especially relevant. In addition to plant growth control, Sentinel-2 will track ground cover shifts and control forests worldwide. It also provides the lakes and coastal waters with emission statistics. Flood images, volcanic eruptions and landslides add to the planning of catastrophes and humanitarian relief efforts [11].

The multispectral imager is carried by Sentinel-2 (shown in Figure 2).This sensor has 13 spectral bands between the sizes of 10 and 60 metres. It has a 10 m resolution in its blue channels (B2), green (B3), red (B4), and close to infrared (B8). Their red edge (B5), NIR (B6, B7 and B8A) and SWIR (B11 and B12) short wave

infrared are all 20 meters long. Finally, its coastal aerosols (B1) and its cirrus (B10) have a pixel scale of 60 meters. [7].

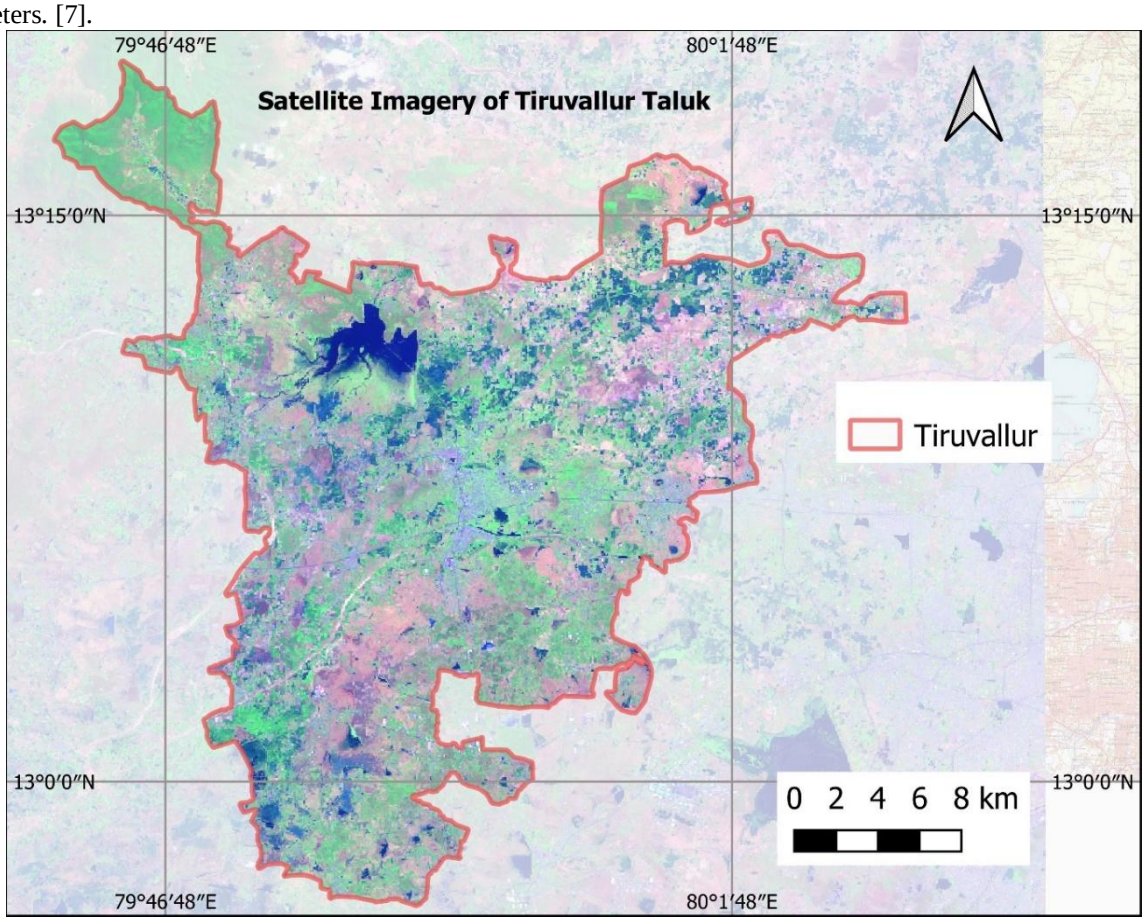

Figure 2: Sentinel Satellite Imagery of Tiruvallur Taluk, Tamil Nadu, India

B. Sentinel Band Combinations

Band variations are used to help explain the characteristics of imaging. The way we do so is by imaginative rearrangement of the existing networks. We may derive such information from an image using band combinations. There are band combinations in a picture that emphasise geological, farming or vegetation characteristics. we should try out the Sentinel Playground if we want to see Sentinel band combos for ourself. It shows the following and some other band variations [5], [6].

C. Natural Colour (B4, B3, B2)

The variation of the natural-coloured band uses the red channels (B4), green (B3) and blue (B2). The aim is to show pictures like we see the world in our eyes. Good foliage is green, just as we see it. Next, urban characteristics frequently look white and grey. Lastly, depending on how safe it is, water is dark blue [12].

D. **Colour Infrared (B8, B4, B3)**

The mixing of colour infrared bands aims to enhance stable and unsafe plants. It is perfect for reflecting chlorophyll by using the near-infrared (B8) line. Therefore, the denser vegetation is red in an infrared colour image. However, there are white urban centres.

E. Short-Wave Infrared (B12, B8A, B4)

The mixing of colour infrared bands aims to enhance stable and unsafe plants. It is perfect for reflecting chlorophyll by using the near-infrared (B8) line. Therefore, the denser vegetation is red in an infrared colour image. However, there are white urban centres.

F. Sentinel 2 Geology (B12, B11, B2)

The mixture of geological strips is an excellent application for geological characteristics. It covers defects, lithology and geology. Geologists appear to use this mix of sentinel bands for study through the use of SWIR-2 (B12), SWIR-1 (B11) and Blue (B2) bands.

G. Bathymetric - (B4, B3, B1)

The combination of bathymetry is suitable for coastal research, as its name suggests. The variation of the bathymetric band uses the red (B4), green (B3) and shore band (B1). It is good to estimate suspended sediments in water by using the coastal aerosol band.

H. Vegetation Index

The vegetational index is appropriate for quantifying the volume of vegetation as near-infrared (vegetation heavily reflects) and red light (vegetation absorbing). Eq is the formula for the standardised vegetation disparity measure (1). While high values indicate dense canopy, low and negative values indicate urban and water characteristics.

NDVI = (B8-B4)/(B8+B4) (1)

I. Moisture Index

The moisture index is suitable to detect tension in plants. It generates moisture content indices using the shortwave and near-infrared. In general, higher values are seen in wetter vegetation. But lower moisture index values indicate that the plants have inadequate humidity under heat. The standardised moisture index formula is given Eq (2).

MI = (B8A-B11)/(B8A+B11) (2)

The NDMI is a distance sensing sensor that is susceptible to water content changes in the leaves. The NDMI is computed with near-infrared reflectance (Sentinel Bank 11) and shortwave infrared reflectance (SWIR - Sentinel Band 11). The NDMI is calculated using the EFFIS Delivery Data Products supplied by the German Aerospace Centre. The ETRS LAEA co-ordinate reference scheme provides MODIS data per tile [13].

IV. RESULTS AND DISCUSSION

The SWIR reflection reflects changes in the water quality of plants and vegetation canopy spongy mesophyll, while the NIR reflection depends not on the water content but the inner leaf structures and leaf dry matter content. The combination of the NIR band with the SWIR band eliminates changes caused by the internal structure and content of the leaves with the dry matter, thus improving the efficiency of the water content recovery for vegetation. The quantity of water available in the internal leaf structure essentially controls the spectral reflectance in the SWIR interval of the electromagnetic spectrum. Therefore, SWIR reflection is damaging to the water content of the leaf. Different studies have shown its utility for tracking drought and early warning [9]. The reflection is calculated using NIR and SWIR, subject to variations in the quality of liquid water and the spongy mesophyll of plant canopy Themes like hydrological hydrographs can comfortably be aggregated with grided data [13]. It makes it necessary to compare the severity and length of NDMI anomalies qualitatively and quantitatively, with registered impacts such as decreases in yield, low flows and lower levels of soil, to name but a few. The NDMI product ranges from -1 to +1, based on the composition of the leaf and vegetation and its cover (Figure 3). Strong NDMI values lead to high water levels in vegetation and high coverage of vegetation. [14] and low NDMI values correlate to low water levels and low fractional coverage of vegetation. NDMI can decrease during the water stress time [15]–[17]. Anomalies of NDVI and NDMI can be seen in table 1 and figure 3&4, giving information on the spatial distribution and temporal progression of vegetation water stress over more extended periods. Subjects such as hydrological watersheds can be conveniently aggregated with grided data. It makes it necessary to compare the severity and length of NDMI anomalies qualitatively and quantitatively, with registered impacts such as decreases in yield, low flows and lower levels of soil, to name but a few. o Dimension of the NDMI product [14].

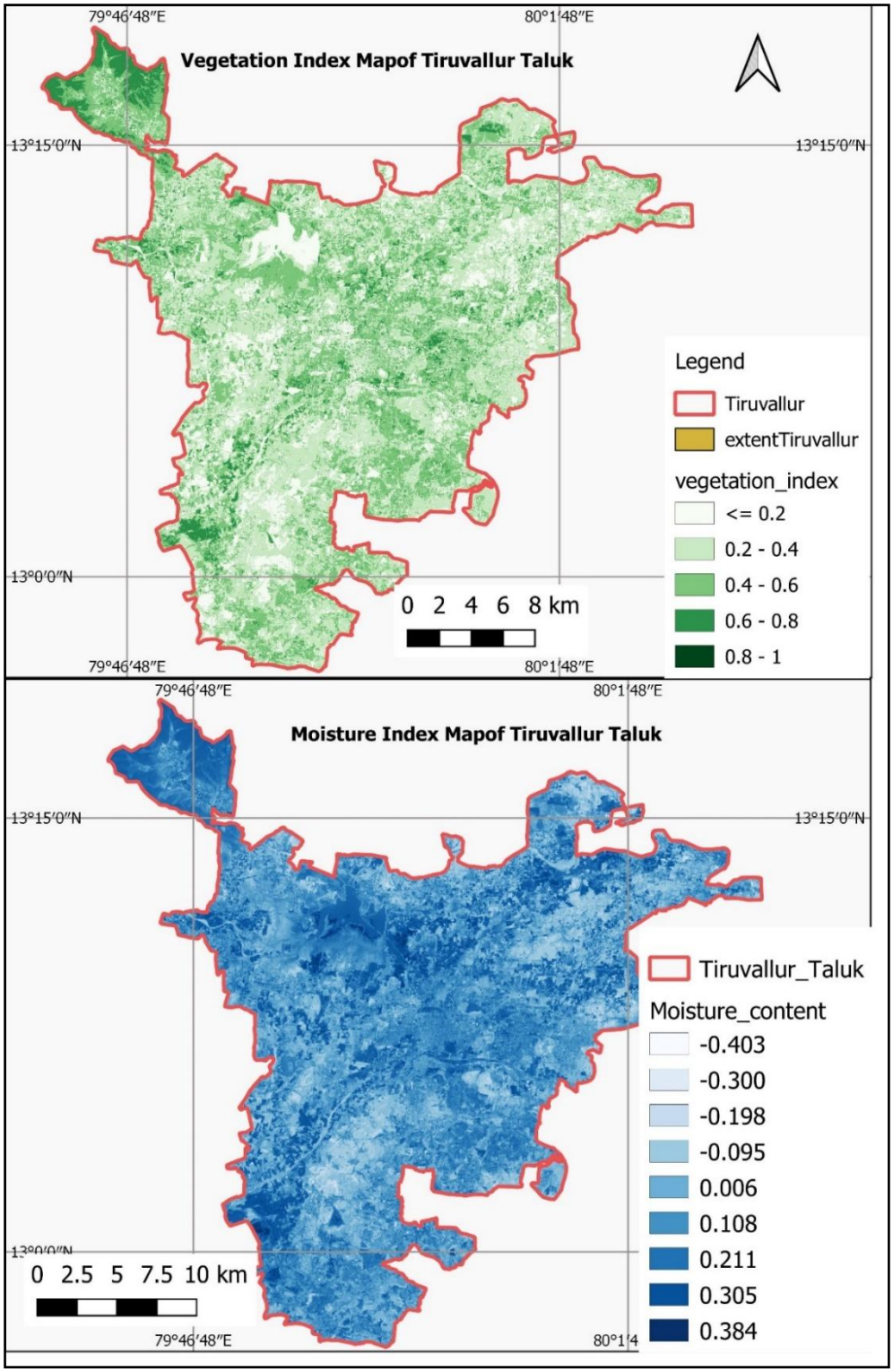

Figure 3: Vegetation index and Moisture index map of Tiruvallur taluk using geospatial technology

Table 1: distribution of area available according to vegetation index and moisture index

Vegetation Index					Moisture Content				
Range	Value	Pixel count	Area (ha)	% area	Range	Value	Pixel count	Area (ha)	% area
0.0 - 0.1	1	192062	1898	2.85	0.0 – 0.1	1	865518	34602	51.94
0.1 - 0.2	2	775041	7661	11.50	0.1 - 0.2	2	479215	19158	28.76
0.2 - 0.3	3	1632062	16134	24.22	0.2 - 0.3	3	298530	11934	17.91
0.3 - 0.4	4	1633018	16143	24.24	0.3 - 0.4	4	22946	917	1.377
0.4 - 0.5	5	1317202	13021	19.55					
0.5 - 0.6	6	860348	8505	12.77					
0.6 - 0.7	7	324995	3212	4.82					
0.7 - 0.8	8	2999	29	0.04					
			66607					66612	

The normalized vegetation differential (NDVI) index is estimated and divided into 8 classes. The Figure 4 shows that the area is covered by 1,698 hectares (2.85 percent) with less than 0.1 of vegetation index while the study area is covered by the vegetation index of 7,661 hectares (11.5 percent) of land. The gradation indicates that the area covering the vegetation index range is 16,134 ha (24,23%), 16,143 ha (24,23%) and 130,021 ha (19,55%). The ranges are 0,2-0,3%, 0,3-0,4%, 0,4-0,5%. The same is said for the description that the region covering the vegetation index spectrum of 0.5-0.6, 0.6-0.7, 0,7-0.8 and 8505 ha (12.77 percent), 3,212 ha (4.82 percent), 29 ha (0,04 percent). The moisture content of the study area divided into four classes as shown in Figure 5. The land area 34602 ha (51.94%), 19158 ha (28.76%) and 11934 ha (17.91%) cover the moisture content of 0.0-0.1, 0.1-0.2, and 0.2-0.3, respectively. The maximum of 917 ha (1.377%) has high amount of moisture content.

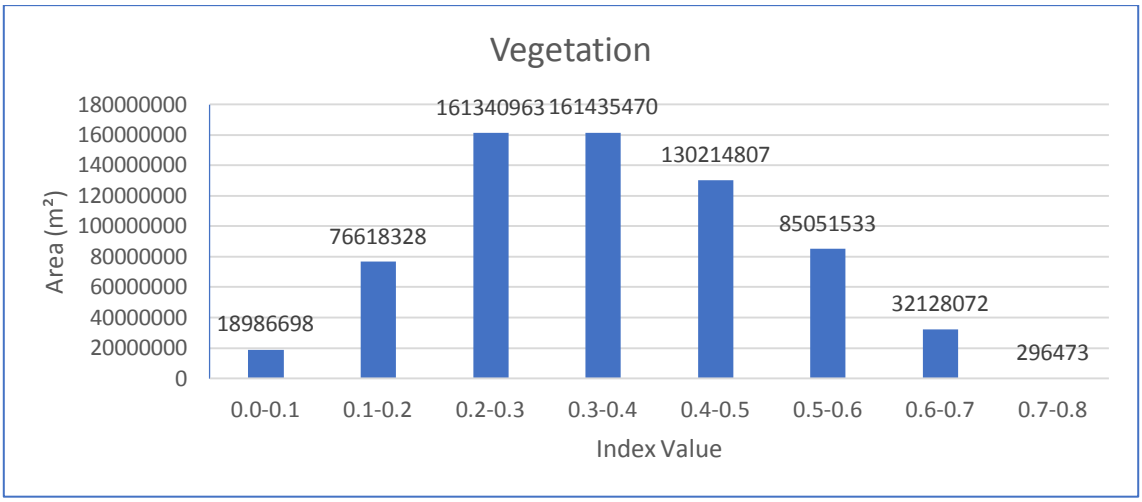

Figure 4: Distribution of area according to Vegetation index

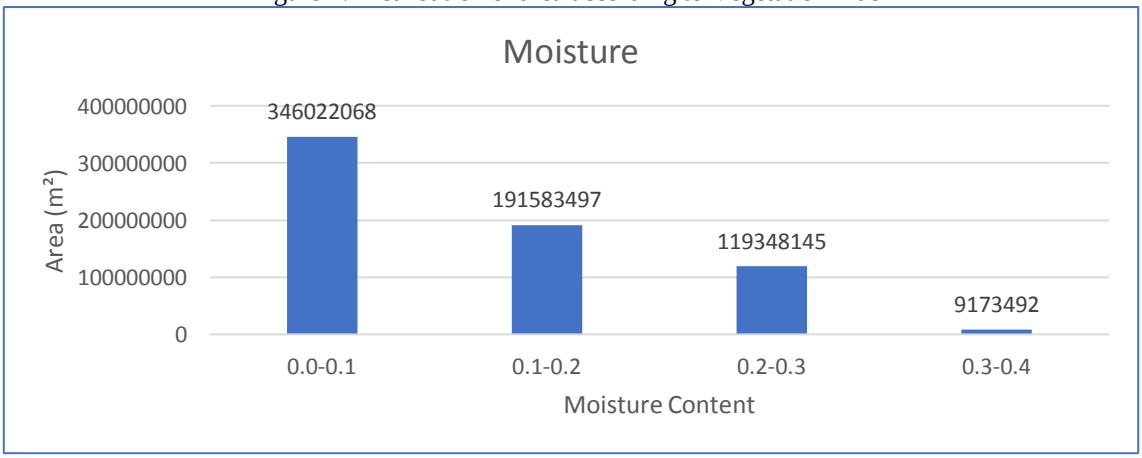

Figure 5: Distribution of area according to Moisture Index

The histogram of normalised difference vegetation index (NDVI) and moisture index are shown in Fig.6 and Fig.7. The expansion of your histogram by using different methods may be improved visually. A graphical image histogram is the pixel count in an image according to its intensity. The more the histogram extends, the more the picture contrasts. However, histogram stretching can also lead to adverse effects on pictures of 8 bits or colours, i.e. visible picture gradient [18]. Therefore, the histogram should be extended on the numerical values of the original grid with single or double precision and converted into an image. Equalisation of areas is another popular technique used for image improvement that contains the same number of pixels for each intensity class [19].

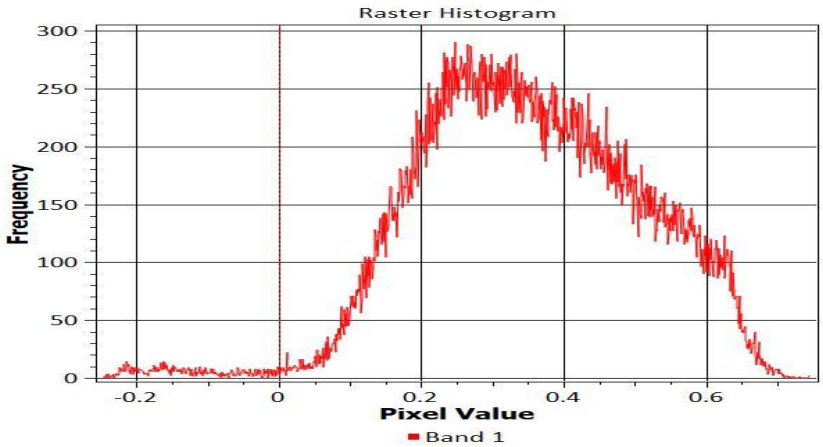

Figure 6: Histogram of distribution of area according to Vegetation Index

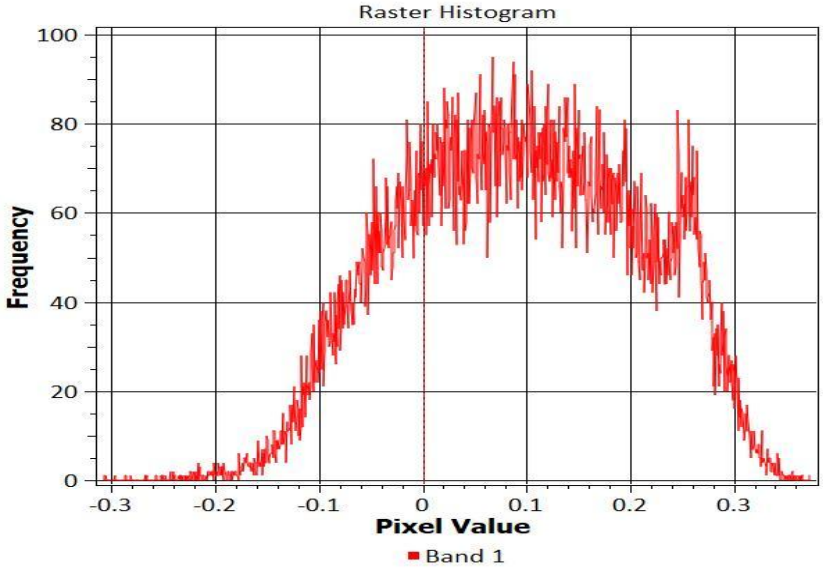

Figure 7: Histogram of distribution of area according to Moisture Index

V. CONCLUSIONS

Gao (1996) states NDMI is a good measure of the liquid content of the vegetation and is less susceptible than NDVI to atmospheric dispersal impacts (Normalized Difference Vegetation Index). The moisture status of vegetative canopies was detected and monitored in a vast region (e.g. Delbart et al. 2005, Jackson et al. 2004) and validated as an indication for drought. Gu et al. (2007) observed that values of NDMI respond faster than NDVI to drought. In contrast to NDMI, NDVI cannot collect information about the vegetation quality of water because NDVI offers information about vegetation greenness (chlorophyll) that is not explicitly and consistently linked. The accord between the actual values of local soil moisture, which cannot, however, be calculated in situ, and the Sentinel figures extracted should be superior to that. In implementations, even in areas with similar climates and soil characteristics, the process shows some promise. For instance, for the parametrisation of the land-surface global circulation models, the awareness of the broad soil moisture area is essential. Currently, soil moisture knowledge is insufficient. Satellite evaluation has significant potential. The ranges are 0,2-0,3%, 0,3-0,4%, 0,4-0,5%. The same is said for the description that the region covering the

vegetation index spectrum of 0.5-0.6, 0.6-0.7, 0,7-0.8 and 8505 ha (12.77 percent), 3,212 ha (4.82 percent), 29 ha (0,04 percent). The moisture content of the study area divided into four classes as shown in Figure 5. The land area 34602 ha (51.94%), 19158 ha (28.76%) and 11934 ha (17.91%) cover the moisture content of 0.0-0.1, 0.1-0.2, and 0.2-0.3, respectively. The maximum of 917 ha (1.377%) has high amount of moisture content.

REFERENCES

[1]. M. Govender, P. J. Dye, I. M. Weiersbye, E. T. F. Witkowski, and F. Ahmed, "Review of commonly used remote sensing and ground-based technologies to measure plant water stress," *Water SA*, vol. 35, no. 5, pp. 741–752, 2009, doi: 10.4314/wsa.v35i5.49201.

[2]. Y. Kim, D. M. Glenn, J. Park, H. K. Ngugi, and B. L. Lehman, "Hyperspectral image analysis for water stress detection of apple trees," *Comput. Electron. Agric.*, vol. 77, no. 2, pp. 155–160, 2011, doi: 10.1016/j.compag.2011.04.008.

[3]. H. E. Nilsson, "Remote sensing and image analysis in plant pathology," *Annu. Rev. Phytopathol.*, vol. 33, pp. 489–527, 1995, doi: 10.1146/annurev.phyto.33.1.489.

[4]. L. Iyappan and P. K. K. Pandian, "Identification of Potential Zone for Wind Farm in Ambasamudram Taluk– A Geospatial Approach," *Int. J. Earth Sci. Eng.*, vol. 5, no. 3, pp. 484–493, 2012.

[5]. M. J. Steinhausen, P. D. Wagner, B. Narasimhan, and B. Waske, "Combining Sentinel-1 and Sentinel-2 data for improved land use and land cover mapping of monsoon regions," *Int. J. Appl. Earth Obs. Geoinf.*, vol. 73, no. April, pp. 595–604, 2018, doi: 10.1016/j.jag.2018.08.011.

[6]. D. P. Roy, H. Huang, L. Boschetti, L. Giglio, L. Yan, and H. H. Zhang, "Landsat-8 and Sentinel-2 burned area mapping - A combined sensor multi-temporal change detection approach," *Remote Sens. Environ.*, vol. 231, no. October 2018, p. 111254, 2019, doi: 10.1016/j.rse.2019.111254.

[7]. D. D. Alexakis, F. D. K. Mexis, A. E. K. Vozinaki, I. N. Daliakopoulos, and I. K. Tsanis, "Soil moisture content estimation based on Sentinel-1 and auxiliary earth observation products. A hydrological approach," *Sensors (Switzerland)*, vol. 17, no. 6, pp. 1–16, 2017, doi: 10.3390/s17061455.

[8]. M. Science, "Water quality as a regional driver of coral biodiversity and macroalgae on the Great Barrier Reef," *Ecol. Appl.*, vol. 20, no. 3, pp. 840–850, 2010.

[9]. H. J. Chu, L. M. Jaelani, M. Van Nguyen, C. H. Lin, and A. C. Blanco, "Spectral and spatial kernel water quality mapping," *Environ. Monit. Assess.*, vol. 192, no. 5, 2020, doi: 10.1007/s10661-020-08271-9.

[10]. K. Toming, T. Kutser, A. Laas, M. Sepp, B. Paavel, and T. Nõges, "First experiences in mapping lakewater quality parameters with sentinel-2 MSI imagery," *Remote Sens.*, vol. 8, no. 8, pp. 1–14, 2016, doi: 10.3390/rs8080640.

[11]. K. Muthu, M. Petrou, C. Tarantino, and P. Blonda, "Landslide Possibility Mapping Using Fuzzy Approaches," *IEEE Trans. Geosci. Remote Sens.*, vol. 46, no. 4, pp. 1253–1265, 2008.

[12]. A. Çöltekin and J. Biland, "Comparing the terrain reversal effect in satellite images and in shaded relief maps: an examination of the effects of color and texture on 3D shape perception from shading," *Int. J. Digit. Earth*, vol. 12, no. 4, pp. 442–459, 2019, doi: 10.1080/17538947.2018.1447030.

[13]. N. Zhang, Z. Gao, X. Wang, and Y. Chen, "Modeling the impact of urbanisation on the local and regional climate in Yangtze River Delta, China," *Theor. Appl. Climatol.*, vol. 102, no. 3, pp. 331–342, 2010, doi: 10.1007/s00704-010-0263-1.

[14]. R. P. Singh, N. Singh, S. Singh, and S. Mukherjee, "Normalized Difference Vegetation Index (NDVI) Based Classification to Assess the Change in Land Use/Land Cover (LULC) in Lower Assam, India," *Int. J. Adv. Remote Sens. GIS*, vol. 5, no. 1, pp. 1963–1970, 2016, doi: 10.23953/cloud.ijarsg.74.

[15]. G. Caradonna, A. Novelli, E. Tarantino, R. Cefalo, and U. Fratino, "A WebGIS Framework for Dissemating Processed," *Reports Geod. Geoinformatics*, vol. 100, pp. 27–38, 2016.

[16]. G. Prasad and M. V. Ramesh, "Spatio-Temporal Analysis of Land Use/Land Cover Changes in an Ecologically Fragile Area—Alappuzha District, Southern Kerala, India," *Nat. Resour. Res.*, vol. 28, pp. 31–42, 2019, doi: 10.1007/s11053-018-9419-y.

[17]. Y. Megahed, P. Cabral, J. Silva, and M. Caetano, "Land Cover Mapping Analysis and Urban Growth Modelling Using Remote Sensing Techniques in Greater Cairo Region—Egypt," *ISPRS Int. J. Geo-Information*, vol. 4, no. 3, pp. 1750–1769, 2015, doi: 10.3390/ijgi4031750.

[18]. M. Shikada, T. Kusaka, Y. Kawata, and K. Miyakita, "Extraction of Characteristic Properties in Landslide Areas Using Thematic Map Data and Surface Temperature," in *Geoscience and Remote Sensing Symposium, 1993. IGARSS'93. Better Understanding of Earth Environment., International. IEEE, 1993.*, 1993, pp. 103–105.

[19]. M. Favalli and A. Fornaciai, "Visualization and comparison of DEM-derived parameters. Application to volcanic areas," *Geomorphology*, vol. 290, pp. 69–84, 2017, doi: 10.1016/j.geomorph.2017.02.029.